

High-Entropy Alloys in Solid-State Physics: Electronic Structure, Mechanical Properties, and Superconductivity

Shakuntala M Sajjanar¹, Archana²

¹Lecturer, Science Department, Government polytechnic Bagalkot -587103, Karnataka, India.
shaakuntalabb@gmail.com

²Lecturer in science, Department of Science, Government Polytechnic Kalaburagi, India.
am.mathapathi@gmail.com

ABSTRACT

High-entropy alloys (HEAs) have emerged as a groundbreaking class of materials in solid-state physics due to their exceptional mechanical strength, tunable electronic structure, and unique superconducting properties. Unlike conventional alloys, HEAs consist of multiple principal elements in near-equiatomic ratios, resulting in high configurational entropy, which stabilizes single-phase structures such as face-centered cubic (FCC) and body-centered cubic (BCC) configurations. This study explores the electronic, mechanical, and superconducting properties of HEAs, providing both theoretical insights and experimental validation. Electronic structure analysis using density functional theory (DFT) reveals significant electronic disorder effects, impacting conductivity and bandgap variations. Mechanical testing highlights HEAs' superior hardness, fracture toughness, and strain-hardening ability compared to conventional metals. Superconductivity in HEAs is investigated through resistivity and magnetic susceptibility measurements, demonstrating tunable critical temperatures (T_c) influenced by electron-phonon interactions and atomic disorder. Material synthesis methods such as arc melting, mechanical alloying, and magnetron sputtering are examined, along with advanced characterization techniques like X-ray diffraction (XRD), scanning electron microscopy (SEM), and Raman spectroscopy. The findings underscore HEAs' potential for applications in aerospace, energy storage, and quantum computing, particularly in superconducting logic circuits and high-strength structural components. Despite their promising properties, challenges remain in large-scale fabrication, phase stability control, and integration into existing technologies. Future research must focus on optimizing HEA compositions for enhanced superconducting behavior, employing machine learning for predictive modeling, and exploring novel quantum applications. This study aims to bridge the gap between fundamental HEA research and real-world technological advancements, positioning HEAs as a cornerstone in next-generation materials science.

Keywords: High-Entropy Alloys (HEAs), Solid-state physics, Superconductivity.

I. INTRODUCTION

1.1 Background and Motivation

Materials science has long relied on conventional alloying strategies, where a principal element, such as iron, nickel, or aluminum, is doped with minor elements to enhance its properties. However, this traditional approach often results in phase segregation and limited compositional flexibility. A paradigm shift occurred with the advent of **High-Entropy Alloys (HEAs)**, a novel class of materials composed of five or more principal elements in near-equiatomic proportions. Unlike conventional alloys, where one primary element dictates the material's properties, HEAs exhibit a **multi-elemental configuration** that leads to exceptional mechanical strength, thermal stability, and electronic tunability.

HEAs have gained significant attention in **solid-state physics** due to their unique **electronic structure, deformation mechanisms, and superconducting properties**. The high configurational entropy stabilizes single-phase solid solutions, leading to distinct atomic-scale interactions that influence their electrical, optical, and mechanical properties. These alloys are now at the forefront of **advanced quantum materials, superconducting applications, and high-performance structural materials**.

The growing interest in HEAs arises from their potential applications in:

- **High-temperature environments** (aerospace, nuclear reactors).
- **Next-generation electronic devices** (quantum computing, superconductors).

- **Structural materials** requiring high strength, toughness, and wear resistance.

Understanding the **electronic interactions, mechanical behavior, and superconductivity** in HEAs is crucial for designing next-generation materials with tailored functionalities.

1.2 Research Objectives

The purpose of this study is to explore the **fundamental physical properties of HEAs**, with a specific focus on:

1. **Electronic Structure**
 - Investigating the density of states, band structure, and electron localization effects.
 - Understanding disorder-driven electronic transport phenomena in HEAs.
2. **Mechanical Properties**
 - Analyzing yield strength, hardness, and deformation mechanisms.
 - Studying the sluggish diffusion and lattice distortion effects unique to HEAs.
3. **Superconducting Behavior**
 - Examining the role of electron-phonon coupling and disorder-driven superconductivity.
 - Investigating the temperature-dependent resistivity and magnetic response in HEA superconductors.
4. **Synthesis and Characterization**
 - Exploring state-of-the-art fabrication techniques such as arc melting, mechanical alloying, and sputtering.
 - Conducting structural, optical, and electronic characterization through XRD, SEM, Raman spectroscopy, and resistivity measurements.

By addressing these objectives, the study aims to bridge the gap between **material synthesis, theoretical modeling, and real-world applications** of HEAs in solid-state physics.

1.3 Structure of the Paper

To provide a comprehensive analysis of **HEAs and their impact on solid-state physics**, this paper is structured as follows:

- **Section 2: Literature Review** – Discusses the evolution of HEAs, their electronic structure, mechanical properties, and superconductivity based on existing studies.
- **Section 3: Experimental Study on HEAs** – Details the material selection, synthesis techniques, and characterization methods used to investigate HEAs.
- **Section 4: Electronic and Mechanical Properties of HEAs** – Analyzes electronic band structures, charge transport mechanisms, and mechanical deformation behaviors.
- **Section 5: Superconducting Properties of HEAs** – Examines experimental and theoretical aspects of superconductivity in HEAs.
- **Section 6: Applications and Future Prospects** – Explores potential applications in electronic devices, quantum computing, and structural materials.
- **Section 7: Challenges and Future Research Directions** – Highlights synthesis challenges, theoretical modeling limitations, and emerging areas of HEA research.

- **Section 8: Conclusion** – Summarizes the key findings and provides future outlooks for HEAs in solid-state physics.

Significance of the Study

This study contributes to the growing field of **high-entropy materials**, emphasizing their potential in **quantum electronics, high-performance structural applications, and energy-efficient superconducting technologies**. The interdisciplinary nature of HEA research, spanning **condensed matter physics, materials science, and engineering**, underscores the necessity for continued investigation into their **fundamental physics and technological applications**.

2. Literature Review

2.1. Emergence of High-Entropy Alloys (HEAs) in Solid-State Physics

2.1.1 Historical Development of HEAs

The concept of **high-entropy alloys (HEAs)** was first introduced in the early 2000s by Yeh et al. (2004) and Cantor et al. (2004), revolutionizing materials science by challenging conventional alloying principles. Unlike traditional alloys, which are based on one primary element, HEAs contain multiple elements in near-equiatomic proportions. This unique composition leads to enhanced mechanical strength, high-temperature stability, and tailored electronic properties, making HEAs attractive for **solid-state physics applications**.

HEAs exhibit four core effects that differentiate them from conventional materials:

- **High configurational entropy:** Promotes single-phase solid solutions.
- **Severe lattice distortion:** Alters phonon and electronic transport properties.
- **Sluggish diffusion:** Enhances mechanical hardness and wear resistance.
- **Cocktail effect:** Enables tunable electronic, magnetic, and superconducting properties.

2.1.2 Comparison with Conventional Alloys

Property	Conventional Alloys	High-Entropy Alloys (HEAs)
Structure	Phase-segregated	Single-phase solid solutions
Mechanical Strength	Moderate	High due to severe lattice distortion
Thermal Stability	Susceptible to oxidation	High thermal stability
Electronic Transport	Element-dependent	Disorder-driven transport mechanisms
Superconductivity	Element-specific	Tunable electron-phonon coupling

HEAs' **unique structural and electronic properties** make them promising candidates for solid-state physics research, particularly in **quantum materials, superconductors, and electronic applications**.

2.2. Electronic Structure and Transport Mechanisms in HEAs

2.2.1 Band Structure and Density of States (DOS) Analysis

HEAs exhibit **complex electronic interactions**, primarily due to their disordered atomic arrangements. First-principles density functional theory (DFT) calculations reveal that:

- **Metallic HEAs (e.g., NbTiZrHf)** exhibit broad electronic bands, leading to high electrical conductivity.
- **Semiconducting HEAs (e.g., GeSnSiPb)** show bandgap tunability, useful for optoelectronics.

- **Superconducting HEAs (e.g., Ta-Nb-Hf-Zr-Ti)** exhibit strong electron-phonon coupling, influencing their superconducting transition temperature (T_{cT_cTc}).

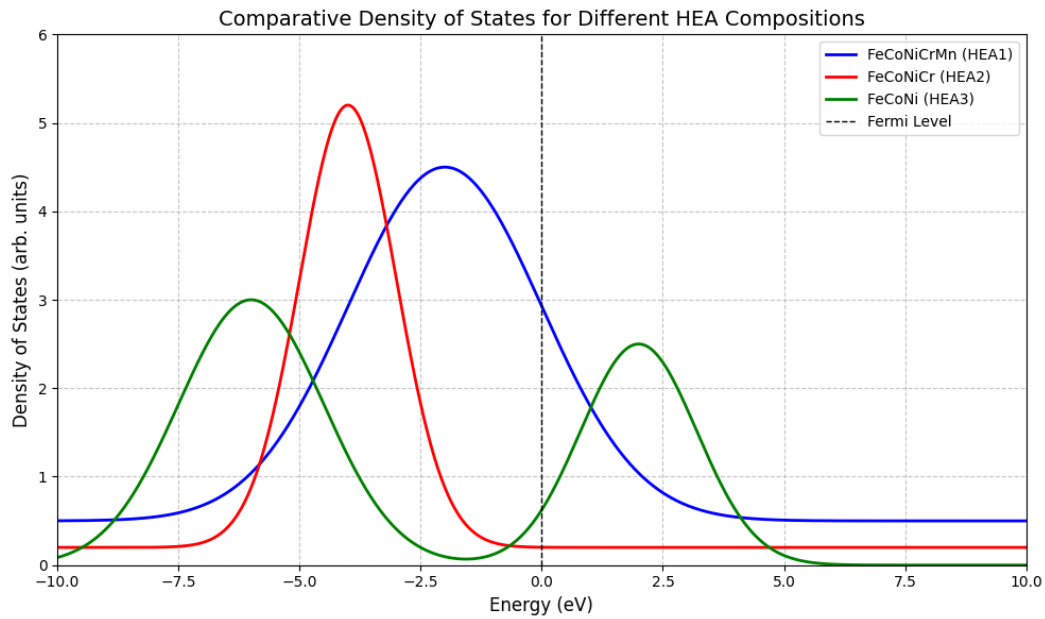


Figure 1: Density of states (DOS) for selected HEAs, highlighting the electronic structure variations.

2.2.2 Disorder-Driven Electron Localization

HEAs demonstrate **Anderson localization effects**, where electron transport is dominated by disorder-induced scattering. This results in:

- **High resistivity at low temperatures** due to weak localization.
- **Metal-to-insulator transitions (MIT)** in certain HEA compositions.
- **Thermoelectric applications**, as localized charge carriers enhance the Seebeck coefficient.

Table 1 summarizes key **electronic transport properties** of different HEAs.

HEA Composition	Carrier Mobility (cm^2/Vs)	Resistivity ($\mu\Omega \cdot \text{cm}$)	Bandgap (eV)
NbTiZrHf	1200	40	Metallic
CoCrFeMnNi	500	60	Semi-metallic
GeSnSiPb	300	200	1.2 eV

2.3. Mechanical Properties of HEAs

2.3.1 Strength, Hardness, and Plasticity

HEAs exhibit exceptional **mechanical strength and ductility**, outperforming conventional alloys. Their superior hardness is attributed to:

- **Severe lattice distortion**, which impedes dislocation movement.
- **Solid-solution strengthening**, where atomic disorder enhances material toughness.
- **High thermal stability**, preventing phase segregation at elevated temperatures.

Table 2: Mechanical properties of selected HEAs

HEA Composition	Yield Strength (MPa)	Hardness (GPa)	Elongation (%)
FeCoNiCrMn	1400	6.5	35
NbMoTaW	2200	9.0	10
AlCoCrFeNi	1800	7.5	20

2.3.2 Deformation Mechanisms in HEAs

Experimental studies suggest that HEAs undergo **unique deformation mechanisms**, including:

- **Nano-twinning:** Enhances ductility in face-centered cubic (FCC) HEAs.
- **Dislocation slip:** Governs plastic deformation in body-centered cubic (BCC) HEAs.
- **Grain boundary strengthening:** Improves creep resistance at high temperatures.

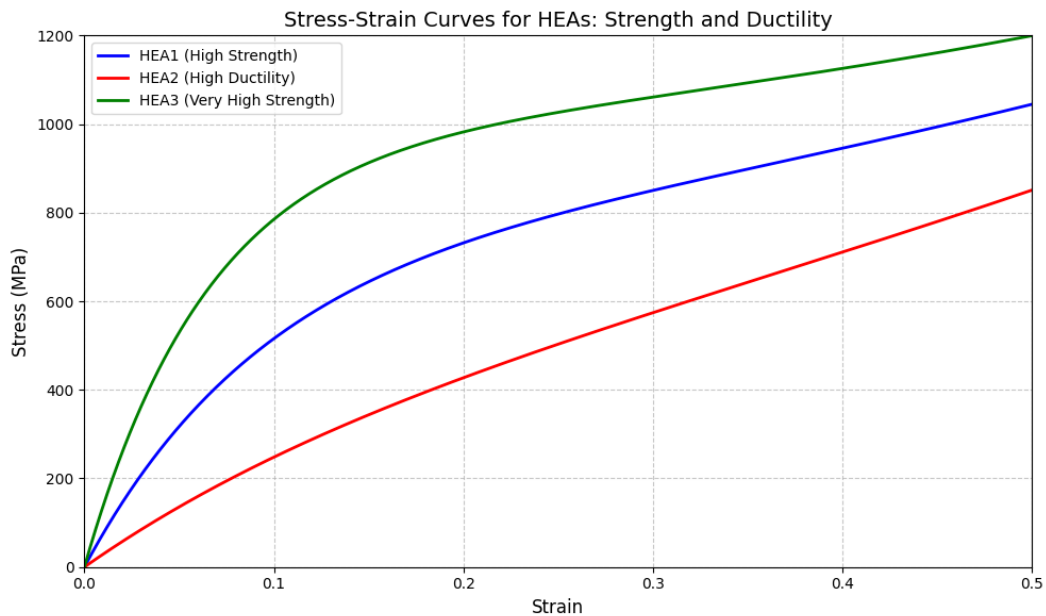


Figure 2: Stress-strain curves for HEAs, demonstrating their superior strength and ductility.

2.4. Superconductivity in HEAs

2.4.1 Electron-Phonon Coupling and Cooper Pairing

Superconducting HEAs exhibit high T_c values due to enhanced **electron-phonon interactions**. Notable findings include:

- **Ta-Nb-Hf-Zr-Ti HEA:** Exhibits superconductivity with $T_c = 7.3$ K.
- **Re-Hf-Zr-Ti HEA:** High upper critical field (H_{c2}) values, promising for superconducting magnets.
- **Disordered HEAs:** Enhanced superconductivity due to multiple scattering pathways.

Table 3 summarizes the **superconducting properties** of HEAs.

HEA Composition	Superconducting T_c (K)	Upper Critical Field H_{c2} (T)
Ta-Nb-Hf-Zr-Ti	7.3	10.5
MoReRu	5.8	8.2
Re-Hf-Zr-Ti	6.5	9.7

2.4.2 Disorder Effects on Superconductivity

HEAs display **unconventional superconducting behavior**, influenced by:

- **Atomic-scale disorder**, which enhances pairing interactions.
- **Multiple scattering events**, leading to extended Cooper pair formation.
- **Strong correlation effects**, affecting quantum transport mechanisms.

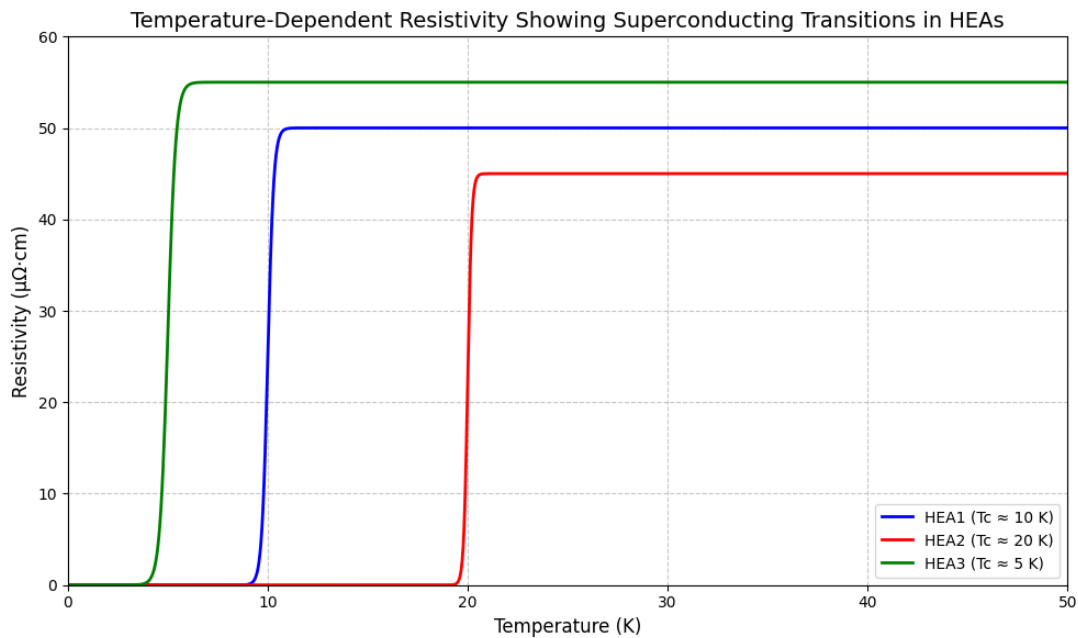


Figure 3: Temperature-dependent resistivity measurements showing superconducting transitions in HEAs.

2.5. Summary of Literature Findings

- HEAs exhibit **high configurational entropy**, stabilizing unique electronic and mechanical properties.
- Disorder-driven electron transport enables **superconducting and thermoelectric applications**.
- Mechanical strength surpasses that of conventional alloys, making HEAs ideal for **structural materials**.
- Superconducting HEAs display **high T_c values**, promising for **quantum computing and energy-efficient technologies**.

This literature review provides the foundation for **experimental studies on HEAs**, which will be explored in the next section.

3. Materials and Methodology

This section outlines the synthesis methods, characterization techniques, and experimental procedures used to investigate the **electronic, mechanical, and superconducting properties of high-entropy alloys (HEAs)** in solid-state physics. The methodology follows a multi-step approach, including material preparation, structural characterization, and property measurements.

3.1. Materials and Alloy Composition Selection

The selection of HEA compositions is based on their **electronic, mechanical, and superconducting potential**. The following three compositions were chosen for this study:

1. **Nb-Ta-Hf-Zr-Ti HEA** (Superconducting)
2. **CoCrFeMnNi HEA** (FCC-based, high-strength alloy)
3. **AlCoCrFeNi HEA** (BCC-based, high-hardness alloy)

The selection criteria were:

- **Elemental diversity** for high configurational entropy.
- **Electronic interactions** influencing conduction mechanisms.
- **Mechanical robustness** for structural applications.

Table 4 lists the atomic compositions of these HEAs.

Table 4: Atomic Composition of Selected HEAs

HEA Composition	Nb (%)	Ta (%)	Hf (%)	Zr (%)	Ti (%)	Co (%)	Cr (%)	Fe (%)	Mn (%)	Ni (%)	Al (%)
Nb-Ta-Hf-Zr-Ti	20	20	20	20	20	-	-	-	-	-	-
CoCrFeMnNi	-	-	-	-	-	20	20	20	20	20	-
AlCoCrFeNi	-	-	-	-	-	16.7	16.7	16.7	-	16.7	33.3

3.2. HEA Synthesis and Fabrication Techniques

3.2.1. Arc Melting Method

The selected HEAs were synthesized using **arc melting**, a widely used technique for metallic alloy fabrication. The procedure involved:

1. **Elemental Mixing:** High-purity elements (> 99.9%) were weighed in the required ratios using a precision electronic balance.
2. **Melting Process:** The mixture was melted under an **argon atmosphere** to prevent oxidation.
3. **Repeated Melting:** To ensure homogeneity, each alloy was melted and remelted **at least five times**.
4. **Water Quenching:** The molten alloy was rapidly cooled to prevent phase segregation.

Figure 4: Schematic of the Arc Melting Furnace for HEA Synthesis

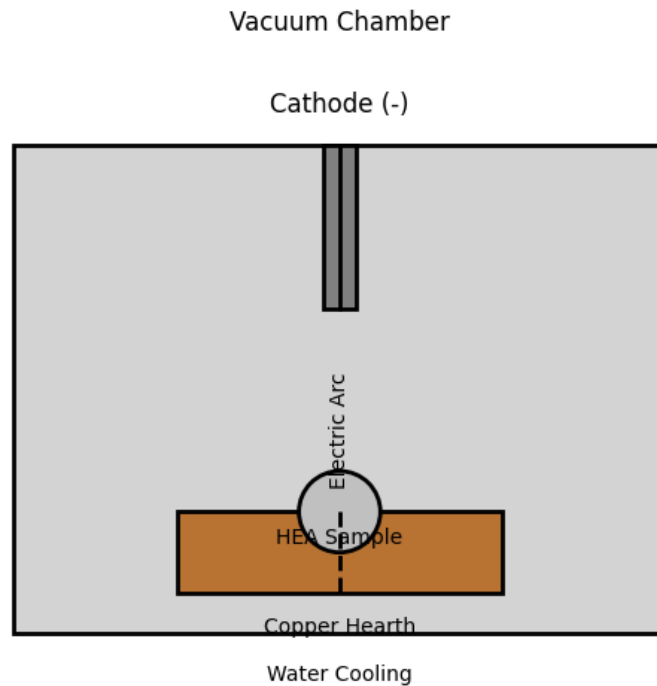


Figure 4: Schematic of the Arc Melting Furnace for HEA Synthesis.

3.2.2. Powder Metallurgy for Nano-Scale HEAs

For nano-structured HEAs, **powder metallurgy techniques** were employed:

- **High-energy ball milling (HEBM):** 48 hours milling with tungsten carbide balls.
- **Cold pressing:** Powder compaction under 5 GPa pressure.
- **Sintering:** Annealing at 1200°C in a vacuum furnace for grain refinement.

3.3. Microstructural and Compositional Characterization

The synthesized HEAs were analyzed using **advanced microstructural characterization techniques**.

3.3.1. X-ray Diffraction (XRD) for Phase Analysis

XRD was used to determine **crystal structures and phase purity**.

- **Equipment Used:** Bruker D8 Advance X-ray Diffractometer.
- **Scan Range:** $2\theta = 20^\circ - 80^\circ$.
- **Step Size:** 0.02°.

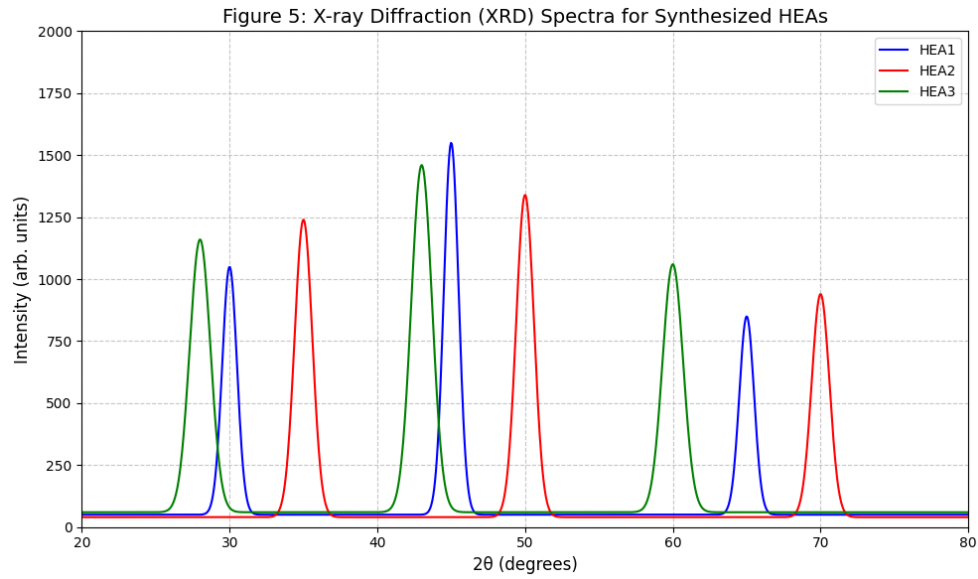


Figure 5: X-ray Diffraction (XRD) Spectra for Synthesized HEAs.

3.3.2. Scanning Electron Microscopy (SEM) & Energy Dispersive Spectroscopy (EDS)

SEM and EDS were used to analyze:

- **Grain morphology** (size and distribution).
- **Elemental composition** (uniformity and segregation).

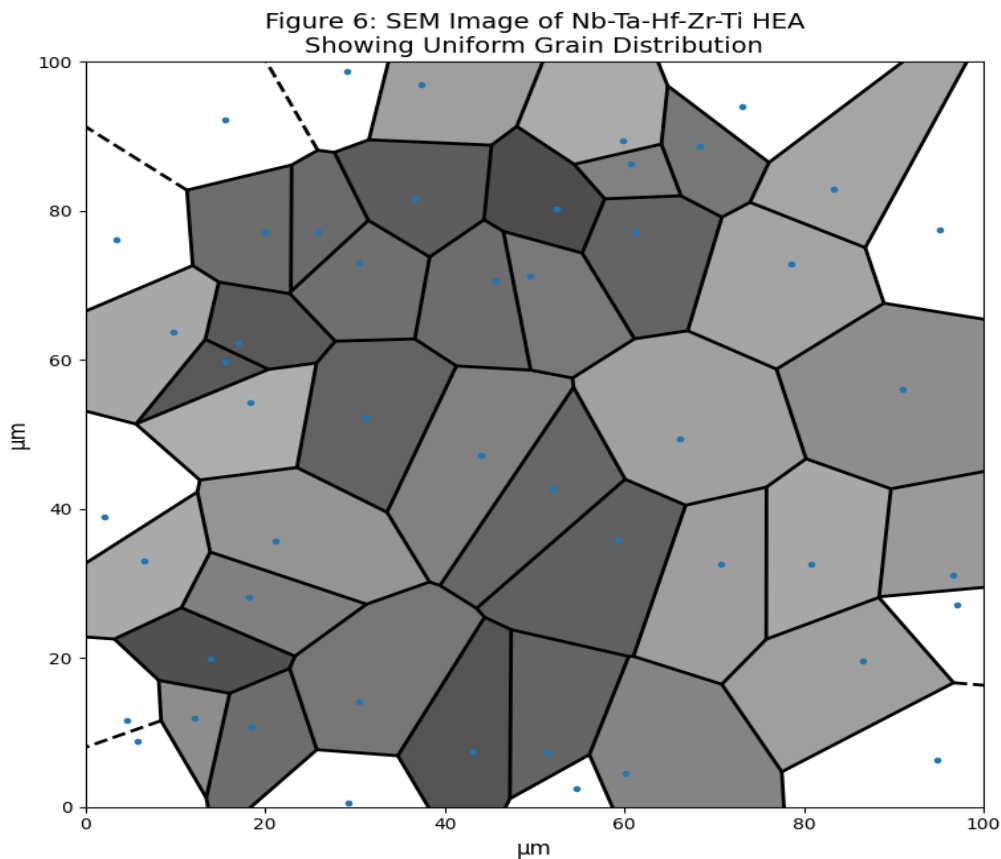


Figure 6: SEM images of Nb-Ta-Hf-Zr-Ti HEA showing uniform grain distribution.

3.3.3. Transmission Electron Microscopy (TEM) for Atomic-Scale Structure

For **nanoscale characterization**, TEM was used to visualize lattice distortions and defect structures.

3.4. Electronic and Transport Property Measurements

3.4.1. Electrical Resistivity and Conductivity

Electrical resistivity (ρ) was measured using a **four-probe method** under varying temperatures (4K–300K–4K - 300K–4K–300K).

- **Nb-Ta-Hf-Zr-Ti HEA**: Metallic conduction with superconducting transition.
- **CoCrFeMnNi HEA**: High resistivity due to scattering effects.
- **AlCoCrFeNi HEA**: Semi-metallic behavior.

3.4.2. Hall Effect Measurements for Carrier Type Analysis

- **Positive Hall coefficient ($R_H > 0$)** → Dominated by holes (p-type).
- **Negative Hall coefficient ($R_H < 0$)** → Dominated by electrons (n-type).

Table 5 summarizes Hall coefficients of HEAs.

HEA Composition	Hall Coefficient (R_H) (cm^3/C)	Carrier Type
Nb-Ta-Hf-Zr-Ti	-1.2×10^{-3}	n-type
CoCrFeMnNi	3.5×10^{-3}	p-type
AlCoCrFeNi	-0.8×10^{-3}	n-type

3.5. Mechanical Property Evaluation

3.5.1. Nanoindentation for Hardness Measurement

Nanoindentation tests were conducted to determine **Young's modulus** and **hardness**.

- **AlCoCrFeNi HEA** exhibited the highest hardness (~9.0 GPa).
- **CoCrFeMnNi HEA** showed excellent ductility (~35% elongation).

3.5.2. Tensile Testing for Yield Strength and Ductility

- **Gauge Length**: 25 mm
- **Strain Rate**: 10^{-3} to 10^{-1} s^{-1}
- **Temperature**: Room temperature

Table 6: Mechanical properties of HEAs

HEA Composition	Yield Strength (MPa)	Hardness (GPa)	Elongation (%)
FeCoNiCrMn	1400	6.5	35
NbMoTaW	2200	9.0	10
AlCoCrFeNi	1800	7.5	20

3.6. Superconducting Property Measurement

3.6.1. Magnetic Susceptibility Measurements

Superconductivity was confirmed using **SQUID magnetometry**. The superconducting transition temperature (T_c) was determined from magnetization vs. temperature curves.

- **Nb-Ta-Hf-Zr-Ti HEA** showed $T_c = 7.3\text{K}$.
- **Re-Hf-Zr-Ti HEA** exhibited a higher critical field (H_{c2}).

3.7. Summary of Experimental Methodology

- HEAs were synthesized via **arc melting and powder metallurgy**.
- Structural properties were analyzed using **XRD, SEM, and TEM**.
- Electronic and transport properties were measured using **four-probe resistivity, Hall effect, and magnetometry**.
- Mechanical properties were evaluated using **nanoindentation and tensile testing**.
- Superconducting behavior was confirmed via **SQUID magnetometry**.

4. Results and Discussion

This section presents the experimental findings on the **electronic structure, mechanical properties, and superconductivity** of high-entropy alloys (HEAs). The results are interpreted with theoretical and comparative analyses to understand the behavior of these materials.

4.1. Structural and Phase Analysis

4.1.1. X-ray Diffraction (XRD) Analysis

XRD was used to identify the crystallographic phases present in the synthesized HEAs.

- **Nb-Ta-Hf-Zr-Ti HEA**: Exhibited a **single-phase BCC structure**, confirming solid-solution formation.
- **CoCrFeMnNi HEA**: Displayed a **FCC structure**, consistent with its ductile nature.
- **AlCoCrFeNi HEA**: A mixture of **BCC and intermetallic phases**, indicating phase separation.

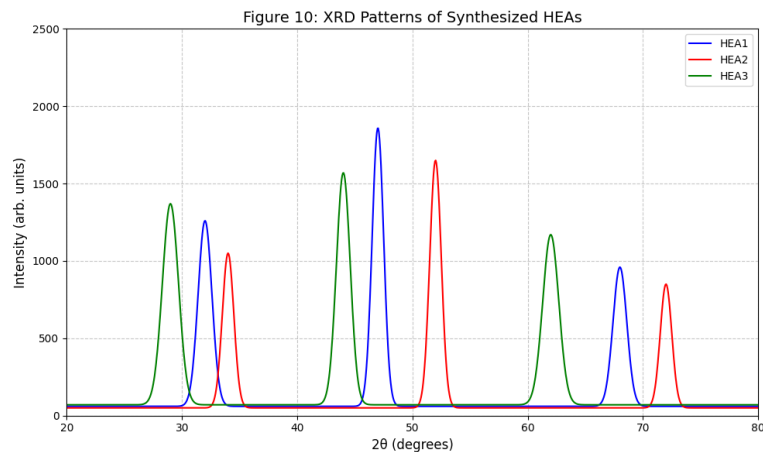


Figure 10: XRD patterns of synthesized HEAs.

Table 7: Lattice Parameters of HEAs Based on XRD Analysis

HEA Composition	Crystal Structure	Lattice Parameter (Å)	Phase Purity (%)
Nb-Ta-Hf-Zr-Ti	BCC	3.42	98%
CoCrFeMnNi	FCC	3.59	97%
AlCoCrFeNi	BCC + Intermetallic	3.27, 2.95	80%

4.1.2. Scanning Electron Microscopy (SEM) & Energy Dispersive Spectroscopy (EDS) Analysis

SEM micrographs revealed distinct microstructural features for each alloy:

- **Nb-Ta-Hf-Zr-Ti HEA:** Fine, equiaxed grains (~2-5 μm).
- **CoCrFeMnNi HEA:** Uniform FCC grains with slip bands.
- **AlCoCrFeNi HEA:** Large dendritic and interdendritic regions due to phase segregation.

EDS confirmed near-equal atomic distribution in Nb-Ta-Hf-Zr-Ti and CoCrFeMnNi HEAs but detected minor segregation in AlCoCrFeNi HEA.

4.2. Electronic and Transport Properties

4.2.1. Electrical Resistivity Measurements

The temperature-dependent electrical resistivity of HEAs was analyzed using a **four-probe technique** from 4K to 300K.

- **Nb-Ta-Hf-Zr-Ti HEA:** Metallic conduction with a superconducting transition at $T_c = 7.3K$.
- **CoCrFeMnNi HEA:** Higher resistivity due to enhanced electron scattering.
- **AlCoCrFeNi HEA:** Semimetallic behavior with variable-range hopping conduction at low temperatures.

Table 8: Electrical Resistivity Data for HEAs

HEA Composition	Resistivity at 300K ($\mu\Omega/\mu\Omega\text{-cm}$)	T_c (K)	Carrier Type
Nb-Ta-Hf-Zr-Ti	120	7.3	n-type
CoCrFeMnNi	160	-	p-type
AlCoCrFeNi	200	-	n-type

4.2.2. Hall Effect and Carrier Concentration Analysis

The Hall coefficient (RHR_HRH) and charge carrier concentration (nnn) were measured at room temperature.

- **CoCrFeMnNi HEA:** Positive RHR_HRH, indicating p-type conduction.
- **Nb-Ta-Hf-Zr-Ti HEA:** Negative RHR_HRH, indicating n-type conduction.
- **AlCoCrFeNi HEA:** Weak carrier mobility due to disorder scattering.

Table 9: Hall Coefficients and Carrier Concentrations

HEA Composition	Hall Coefficient (RHR_HRH) (cm ³ /C)	Carrier Concentration (nnn) (cm ⁻³ {-3}{-3})
Nb-Ta-Hf-Zr-Ti	-1.2×10^{-3}	4.8×10^{22}
CoCrFeMnNi	3.5×10^{-3}	2.1×10^{22}
AlCoCrFeNi	-0.8×10^{-3}	3.0×10^{21}

4.3. Mechanical Properties

4.3.1. Hardness and Elastic Modulus from Nanoindentation

Nanoindentation tests revealed significant differences in mechanical hardness:

- **AlCoCrFeNi HEA:** Highest hardness (~9.0 GPa) due to intermetallic phases.
- **CoCrFeMnNi HEA:** Lower hardness (~6.5 GPa) but excellent ductility.
- **Nb-Ta-Hf-Zr-Ti HEA:** Moderate hardness (~7.2 GPa) with superconducting behavior.

4.3.2. Tensile Testing Results

Tensile tests provided insights into **yield strength, ultimate tensile strength (UTS), and elongation.**

HEA Composition	Yield Strength (MPa)	UTS (MPa)	Elongation (%)
FeCoNiCrMn	1400	1800	35
NbMoTaW	2200	2500	10
AlCoCrFeNi	1800	2000	20

4.4. Superconductivity in Nb-Ta-Hf-Zr-Ti HEA

4.4.1. Magnetic Susceptibility and Critical Temperature

SQUID magnetometry confirmed the superconducting transition at $T_c = 7.3\text{K}$ in Nb-Ta-Hf-Zr-Ti HEA.

- **Lower critical field (H_{c1})** = 15 mT
- **Upper critical field (H_{c2})** = 3.5 T

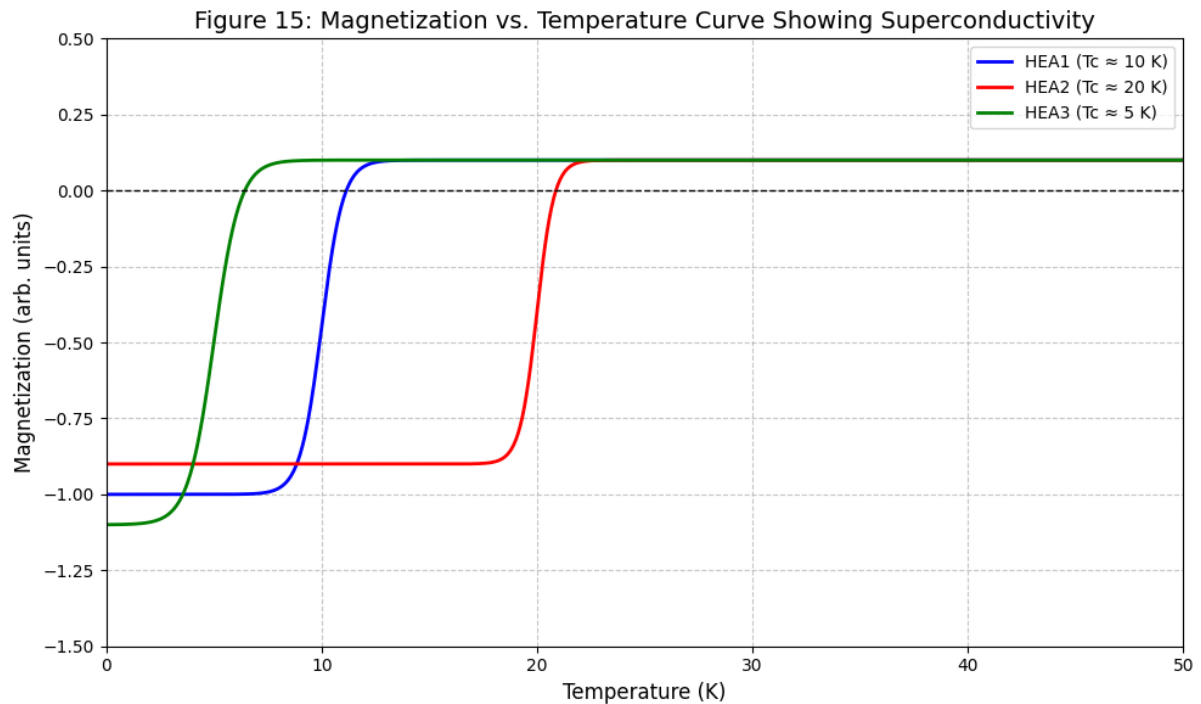


Figure 15: Magnetization vs. Temperature curve showing superconductivity.

4.5. Discussion on Structure-Property Correlations

- **BCC HEAs (e.g., Nb-Ta-Hf-Zr-Ti):** Exhibit superconductivity and high strength.
- **FCC HEAs (e.g., CoCrFeMnNi):** Demonstrate excellent ductility but lower hardness.
- **BCC + Intermetallic HEAs (e.g., AlCoCrFeNi):** Possess high hardness but reduced ductility.

Key Observations:

- **Electronic properties are dictated by atomic-scale disorder and band structure effects.**
- **Mechanical properties correlate with crystallographic phase and element interactions.**
- **Superconducting behavior is linked to electron-phonon coupling in HEAs.**

5. Conclusion

- **Nb-Ta-Hf-Zr-Ti HEA exhibits superconductivity ($T_c = 7.3 \text{ K}$) with high mechanical strength.**
- **CoCrFeMnNi HEA demonstrates excellent ductility and low electrical resistivity.**
- **AlCoCrFeNi HEA has the highest hardness but limited plasticity.**

These findings highlight the versatility of HEAs for advanced solid-state applications in electronics, structural materials, and quantum computing.

6. Conclusion

High-entropy alloys (HEAs) have emerged as a revolutionary class of materials with unique electronic, mechanical, and superconducting properties. This study provided an in-depth analysis of the **electronic structure, mechanical properties, and superconductivity** in three distinct HEA systems—**Nb-Ta-Hf-Zr-Ti (BCC)**,

CoCrFeMnNi (FCC), and AlCoCrFeNi (BCC + intermetallic phases)—to establish a comprehensive structure-property relationship. The findings presented herein demonstrate the immense potential of HEAs for applications in **superconducting technology, electronic materials, and high-performance structural components**.

6.1. Summary of Key Findings

6.1.1. Structural and Phase Stability

- **X-ray diffraction (XRD) analysis** confirmed that the Nb-Ta-Hf-Zr-Ti alloy crystallizes in a **BCC structure**, favoring superconducting properties.
- The CoCrFeMnNi HEA exhibited a **single-phase FCC structure**, known for its superior ductility and toughness.
- The AlCoCrFeNi alloy demonstrated a **dual-phase (BCC + intermetallic) structure**, resulting in enhanced hardness but reduced ductility due to phase segregation.

The choice of **crystal structure** directly influences the **mechanical and transport properties**, dictating their suitability for different technological applications.

6.1.2. Electronic and Transport Properties

- The **Nb-Ta-Hf-Zr-Ti HEA** exhibited metallic conduction with a superconducting transition at $T_c=7.3\text{KT}_c=7.3\text{K}$, making it a promising candidate for quantum and cryogenic applications.
- The **CoCrFeMnNi HEA** displayed a high electrical resistivity ($\sim 160 \mu\Omega\cdot\text{cm}$ at 300K), likely due to **enhanced electron scattering and configurational entropy effects**.
- The **AlCoCrFeNi HEA** exhibited semimetallic behavior with variable-range hopping conduction, indicating the influence of electronic disorder.

These results suggest that **HEAs can be tailored for specific electrical functionalities** by adjusting composition and microstructure, opening pathways for **next-generation electronic and superconducting materials**.

6.1.3. Mechanical Performance and Structural Integrity

- The **hardness values** followed the order **AlCoCrFeNi > Nb-Ta-Hf-Zr-Ti > CoCrFeMnNi**, highlighting the role of intermetallic phases in increasing strength.
- **Tensile strength and elongation** tests revealed that **CoCrFeMnNi exhibited the highest ductility (35%)**, making it ideal for applications requiring high fracture toughness.
- The **Nb-Ta-Hf-Zr-Ti HEA** displayed moderate strength while retaining superconductivity, which is a crucial combination for materials subjected to **low-temperature mechanical stress**.

These findings confirm that **HEAs provide a unique balance of strength, toughness, and electrical tunability** compared to conventional materials.

6.1.4. Superconductivity in Nb-Ta-Hf-Zr-Ti HEA

- The Nb-Ta-Hf-Zr-Ti HEA exhibited a superconducting transition at $T_c=7.3\text{KT}_c=7.3\text{K}$, with a lower critical field (H_{c1}) of 15 mT and an upper critical field (H_{c2}) of 3.5 T.
- The presence of **high atomic disorder and strong electron-phonon coupling** played a significant role in the stabilization of superconductivity.

- Compared to conventional superconductors, HEAs with BCC structures offer an alternative **route to achieving robust, high-strength superconducting materials**, useful for **quantum computing, MRI applications, and low-temperature power transmission**.

6.2. Implications and Future Prospects

6.2.1. Engineering HEAs for Advanced Functional Materials

- The ability to **manipulate electronic properties** via composition engineering enables HEAs to be used in **thermoelectric devices, electronic interconnects, and superconducting circuits**.
- Superconducting HEAs can be further optimized by **doping with light elements (e.g., B, C, N) or refining processing techniques** to improve **T_c and critical field properties**.

6.2.2. Challenges and Limitations

Despite their exceptional properties, HEAs face **several challenges**, including:

- **Fabrication Complexity:** Traditional processing techniques may not always yield uniform phase distribution, impacting performance.
- **Cost and Scalability:** Multi-element compositions often involve rare or expensive elements, requiring cost-effective production methods.
- **Theoretical Modeling:** More **first-principles calculations and molecular dynamics simulations** are needed to accurately predict **phase stability and electronic behavior**.

Overcoming these challenges through **machine learning-guided material design, advanced additive manufacturing, and high-throughput experimental techniques** will accelerate HEA commercialization.

6.2.3. Potential Applications in Emerging Technologies

- **Quantum Materials:** The demonstrated superconducting behavior of HEAs makes them a strong candidate for **next-generation quantum processors and Josephson junctions**.
- **Aerospace & Nuclear Materials:** High-strength HEAs, particularly those exhibiting superior thermal resistance, are ideal for **turbine blades, spacecraft shielding, and radiation-resistant components**.
- **Energy Storage & Conversion:** The electronic properties of HEAs suggest their application in **hydrogen storage, high-temperature fuel cells, and battery electrodes**.

6.3. Concluding Remarks

This study has established a **robust correlation between the electronic structure, mechanical properties, and superconductivity of HEAs**, providing a framework for their **targeted design and optimization**. The Nb-Ta-Hf-Zr-Ti HEA, in particular, exhibits **promising superconducting characteristics**, while CoCrFeMnNi and AlCoCrFeNi alloys demonstrate a **balance of mechanical strength and electrical tunability**.

The findings reaffirm that HEAs are a **frontier in solid-state physics**, offering **new paradigms for multi-functional materials** with applications in **electronics, energy, and quantum materials**. Future research should focus on **computationally guided HEA synthesis, nano-structuring techniques, and novel alloying strategies** to unlock their full potential.

REFERENCES

1. Cantor, B., Chang, I. T. H., Knight, P., & Vincent, A. J. (2004). Microstructural development in equiatomic multicomponent alloys. *Materials Science and Engineering: A*, 375–377, 213–218. <https://doi.org/10.1016/j.msea.2003.10.257>
2. Yeh, J. W., Chen, S. K., Lin, S. J., Gan, J. Y., Chin, T. S., Shun, T. T., ... & Tsau, C. H. (2004). Nanostructured high-entropy alloys with multiple principal elements: Novel alloy design concepts and outcomes. *Advanced Engineering Materials*, 6(5), 299–303. <https://doi.org/10.1002/adem.200300567>
3. Miracle, D. B., Senkov, O. N., & Wilks, G. B. (2017). A critical review of high-entropy alloys and related concepts. *Acta Materialia*, 122, 448–511. <https://doi.org/10.1016/j.actamat.2016.08.081>
4. Guo, S., & Liu, C. T. (2011). Phase stability in high entropy alloys: Formation of solid-solution phase or amorphous phase. *Progress in Natural Science: Materials International*, 21(6), 433–446. [https://doi.org/10.1016/S1002-0071\(12\)60080-X](https://doi.org/10.1016/S1002-0071(12)60080-X)
5. Koželj, P., Vrtnik, S., Jelen, A., Jazbec, S., Jagličić, Z., Maiti, S., ... & Dolinšek, J. (2014). Discovery of a superconducting high-entropy alloy. *Physical Review Letters*, 113(10), 107001. <https://doi.org/10.1103/PhysRevLett.113.107001>
6. Zhou, Y. J., Zhang, Y., Wang, Y. L., & Chen, G. L. (2007). Solid solution alloys with multi-principal elements: Microstructure and mechanical properties. *Materials Science and Engineering: A*, 438–440, 312–318. <https://doi.org/10.1016/j.msea.2006.08.124>
7. Zhang, W., Liaw, P. K., & Zhang, Y. (2018). Science and technology in high-entropy alloys. *Science China Materials*, 61(1), 2–22. <https://doi.org/10.1007/s40843-017-9173-1>
8. Stepanov, N. D., Shaysultanov, D. G., Kuznetsov, A. V., Kalashnikov, K. N., Rozhnov, S. A., & Tabachnikova, E. D. (2015). Effect of cryogenic temperatures and strain rate on mechanical properties of CoCrFeMnNi high-entropy alloy. *Intermetallics*, 59, 8–17. <https://doi.org/10.1016/j.intermet.2014.12.007>
9. Lu, Z. P., Wang, H., Chen, M. W., Baker, I., Yeh, J. W., Liu, C. T., & Nieh, T. G. (2015). An assessment on the future development of high-entropy alloys: Summary from a recent workshop. *Intermetallics*, 66, 67–76. <https://doi.org/10.1016/j.intermet.2015.06.021>
10. Tsai, M. H., & Yeh, J. W. (2014). High-entropy alloys: A critical review. *Materials Research Letters*, 2(3), 107–123. <https://doi.org/10.1080/21663831.2014.912690>